DOI: 10.19884/j.1672-5220.202408001

All-Cellulose Composites Fabricated by Partially Dissolving Wood Pulp in Cryogenic Aqueous Phosphoric Acid

METASEBIA Gizaw[1], WANG Bijia[1,2*], FENG Xueling[1,2], RONG Liduo[1,2]
1. College of Chemistry and Chemical Engineering, Donghua University, Shanghai 201620, China
2. National Engineering Research Center for Dyeing and Finishing of Textiles, Donghua University, Shanghai 201620, China

Abstract: All-cellulose composites (ACCs) are composites that use non-derivatized cellulose as both the matrix and the reinforcement phase. ACC consists entirely of cellulose, and since the reinforcement phase and the matrix have exactly the same chemical properties, they can overcome the problem of poor fiber-matrix adhesion in biocomposites. In this study, ACC was prepared by partially dissolving wood pulp in a cryogenic aqueous phosphoric acid solution, and the effects of dissolution temperature, dissolution time and pressing load on the properties of ACC were investigated. The results showed that a dissolution time of 45 min achieved the optimal reinforcement-matrix ratio. The use of an aqueous ethanol solution at an ethanol mass fraction of 50% as a coagulation bath and a pressing load of 3 000 kg during the drying process achieved the best mechanical properties of ACC, with a tensile strength of 49.3 MPa (approximately 210% higher than that of the untreated wood pulp) and an elastic modulus of 1.6 GPa (approximately 122% higher than that of the untreated wood pulp). The composite's compactness affected ACC's mechanical properties. The air permeability analysis showed that the barrier performance of ACC was also significantly better than that of the untreated wood pulp. With a pressing load of 3 500 kg, the surface water contact angle (WCA) increased to 110.3° (approximately 94% higher than that of the untreated wood pulp), and the air permeability was significantly reduced to 1.1 mm/s, showing its good application prospects in the field of green packaging materials.

Keywords: cellulose; all-cellulose composite (ACC); cryogenic phosphoric acid; partial dissolution (PD); sustainable material
CLC number: TB332 **Document code**: A
Article ID: 1672-5220(2025)04-0380-11

Open Science Identity (OSID)

0 Introduction

The production of petroleum-derived materials and glass fibers leads to the emission of significant greenhouse gases into the atmosphere. Cellulose is the most prevalent biopolymer on the earth. It is an inexhaustible raw material that may satisfy the growing demand for biocompatible and ecologically benign products among all biomass resources[1-3]. Cellulose fibers are potential reinforcing materials due to their numerous benefits. These benefits include ready availability, light weight, renewability, biocompatibility, biodegradability, low cost, chemical stability, low abrasiveness and excellent mechanical properties[4-6]. Nishino et al.[7] developed the idea of all-cellulose composites (ACCs) which were motivated by the advancement of self-reinforced composites. ACCs use the same polymers for the matrix and reinforcement, which helps solve the problems of poor compatibility and recyclability common in traditional composites. ACCs produce a high-performance biocomposite due to a strong cellulosic reinforcement phase and good interfacial interactions[8].

Two main approaches have been shown for manufacturing ACCs. The first approach involves partially dissolving cellulose fibers to create a matrix phase by immersing them in a solvent that binds the undissolved cellulose fiber cores together. This approach produces reinforcing components because the matrix and reinforcement are made from the same cellulose material. The matrix covers an undissolved reinforcement phase after regeneration. The second approach involves fully dissolving cellulose fibers by using a suitable solvent and conventional impregnation method (CIM) to reinforce the fibrous cellulose material. For the matrix and reinforcement phase, different kinds of cellulose can be used. Both approaches are feasible, but in terms of prospective industrial upscaling, the partial dissolution (PD) approach appears more likely to occur. This is because the triggered shrinkage is lower for ACCs manufactured using the PD approach than that using the CIM[9-11].

The advantage of ACCs is that they are sustainable materials and good for the earth. Since the mixture comprises only cellulose, ACCs can be composted

Received date: 2024-08-02
Foundation item: Fundamental Research Funds for the Central Universities, China (No. 2232023G-04)
* Correspondence should be addressed to WANG Bijia, email: bwang@dhu.edu.cn
Citation: METASEBIA G, WANG B J, FENG X L, et al. All-cellulose composites fabricated by partially dissolving wood pulp in cryogenic aqueous phosphoric acid [J]. *Journal of Donghua University (English Edition)*, 2025, 42(4): 380-390.

without harming the environment or recycled by recovering energy after their useful life. Different cellulose solvents and anti-solvents have been used to process ACCs. *N*-methylmorpholine *n*-oxide (NMMO), LiCl/*N*, *N*-dimethylacetamide (DMAc), ionic liquids (ILs) and aqueous NaOH/urea solutions are the most common solvents[9]. Phosphoric acid can dissolve cellulose derived from various sources, with a degree of polymerization (DP) ranging from 200 (microcrystalline cellulose (MCC)) to 2 200 (cotton fiber) to produce solutions containing cellulose mass concentrations of up to 18%. The dissolving of cellulose in aqueous phosphoric acid, which is efficient, non-derivative and non-destructive, was achieved for the first time by pre-cooling the solution to sub-zero temperatures[12]. Anti-solvents (coagulation mediums) like water, ethanol, acetone, methanol or acetonitrile are often added to precipitate the cellulose[13-15]. Zhu et al.[14] investigated the effects of various anti-solvents on the properties of cellulose regenerated from 1-ethyl-3-methylimidazolium acetate solution, and found that anti-solvents had a critical function in regulating the regenerated cellulose's structure and properties.

Phosphoric acid effectively dissolves cellulose from various sources[16-17]. Phosphoric acid is non-toxic, non-volatile, manageable and reasonably priced. It is a viable option for use as a cellulose solvent. Despite these potential advantages, there is a research gap in using the cryogenic phosphoric acid dissolution method in ACCs. Hence, this study used the cryogenic phosphoric acid PD approach to make wood pulp ACCs. The impact of varying dissolution and regeneration conditions on the composite formation and fiber-matrix interaction was investigated via Fourier transform infrared (FTIR) spectroscopy, X-ray diffraction (XRD) and scanning electron microscopy (SEM) analysis. The properties of the resulting ACCs, including mechanical property, thermal stability, surface hydrophobicity and air permeability, were also studied.

1 Materials and Methods

1.1 Materials

Wood pulp was purchased from Xinxiang Natural Chemical Co., Ltd., China. Phosphoric acid (H_3PO_4, mass fraction of 85%,) was supplied by Shanghai Titan Technology Co., Ltd., China. Ethanol (EtOH, mass fraction of 99%) was purchased from Sinopharm Chemical Reagent Co., Ltd., China. Unless otherwise stated, the materials utilized in this study were not further purified.

1.2 Preparation of ACCs from wood pulp

The preparation of ACCs is shown in Fig. 1. To prepare the ACCs, aqueous H_3PO_4 with a mass fraction of 85% was prepared at three different temperatures: 25, 0 and −18 ℃. Before use, the wood pulp was conditioned for at least 24 h at 23 ℃ and a relative humidity of 50%. To achieve a cellulose mass fraction of 6%, 10.5 g of wood pulp was immersed in 164.5 g of aqueous H_3PO_4 pre-conditioned to the designated temperature and stored for different dissolution time (15, 30, 45 and 60 min) and maintained at the designated temperature during the dissolution process. The partially dissolved wood pulp was transferred to a Teflon mold (15 cm × 15 cm × 1 cm), covered in polyimide (PI) films, and then cold-pressed (200 kg, 3 min). The composites were immersed in the proper coagulation bath. The coagulation baths were composed of 100% deionized water, 50/50 water-ethanol and 100% ethanol, respectively. The composites were washed repeatedly until their surfaces showed a neutral pH value. The ACCs were obtained by hot pressing at 2 000, 2 500, 3 000 and 3 500 kg for 8 h at 90 ℃, followed by conditioning at 23 ℃ and a relative humidity of 50% before characterization.

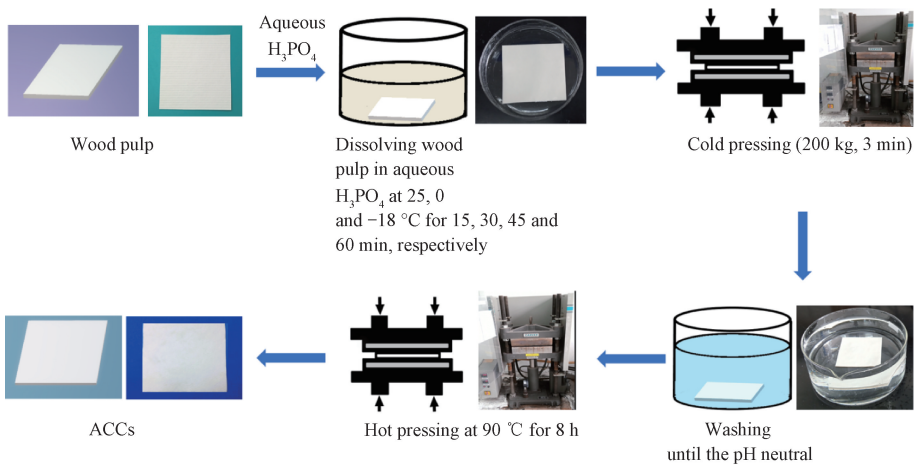

Fig. 1 Preparation of ACCs by PD of wood pulp in aqueous H_3PO_4

1.3 Characterizations

1.3.1 Structural analysis

An FTIR spectrophotometer (Spectrum Two, PERKIN-ELMER, USA) was used to measure the structure of ACCs. The measurements were conducted to acquire all spectra within a range of 400–4 000 cm^{-1} at a resolution of 2 cm^{-1}.

1.3.2 Elemental distribution

Elemental distribution mapping of the ACCs by energy dispersive X-ray spectroscopy (EDS) was conducted by using a scanning electron microscope (SU8010, Hitachi, Japan). The accelerating voltage was set at 15 kV.

1.3.3 Micromorphological analysis

The surface and cross-section of the ACCs were examined with a scanning electron microscope (TM3030, Hitachi, Japan). The cross-sectional morphology was seen after breaking the sample in liquid nitrogen. The cross-section and surface of the sample were covered with a thin layer of gold before inspection. The accelerating voltage was set at 15 kV.

1.3.4 Crystallinity analysis

An X-ray diffractometer (DX-2700BH, Haoyuan, China) was used to gather the XRD patterns of the composites. Each sample was levelled and placed in the sample holder to provide consistent exposure to a monochromatic Cu-Kα radiation ($\lambda = 1.5419 \times 10^{-10}$ m, 40 kV, 40 mA) at room temperature.

The crystallinity of ACCs immersed in aqueous H_3PO_4 is

$$X_c = \frac{A_c}{(A_c + A_a)} \times 100\%, \quad (1)$$

where A_a is the area of the amorphous peak; A_c is the area of the crystalline peak; X_c is the crystallinity.

The crystallite size of the XRD data was calculated by using Scherrer's equation:

$$D = \frac{k\lambda_0}{\beta\cos\theta}, \quad (2)$$

where D is the crystallite size; λ_0 is a constant, and $\lambda_0 = 1.5418 \times 10^{-10}$ m; β represents the corrected integral width; k is the Scherrer's constant, which is 0.94; θ is the Bragg angle.

1.3.5 Thermogravimetric (TG) analysis

TG analysis of the ACCs was carried out by using a TG 209 F3 analyzer (NETZSCH, Germany). It was conducted over a temperature range of 30–900 ℃ in a nitrogen atmosphere at a heating rate of 10 ℃/min. The derivative TG (DTG) data was used to calculate the mass loss rate.

1.3.6 Mechanical properties

The mechanical properties of ACCs were measured according to the GB/T 1040.3—2006 standard. A 500 N load cell-equipped UH6502 universal testing machine (UH Measurement & Control, China) was used to record the mechanical parameters of the manufactured ACCs at room temperature and an extension rate of 5 mm/min. Each sample's dimensions were 5 mm in width and 100 mm in length, with a 20 mm gap between each pair of clips. Every sample was measured at 50% relative humidity and 25 ℃. The ACCs' elongation at break, tensile strength and elastic modulus were measured. Five measurements were taken, and the average result was noted.

1.3.7 Water contact angle (WCA)

The WCA of ACCs was measured by using a T200 contact angle meter (Theta, Finland). For testing, double-sided adhesive tapes were used to secure the ACCs on a glass slide. The WCA was measured with the help of 10 μL of deionized water drops.

1.3.8 Air permeability

The air permeabilities of ACC films were determined by using a YG461E air permeability tester (Wenzhou Fangyuan Instrument Co., China). The GB/T 5453—1997 standard was followed in the preparation of the samples. Every sample was measured at a 65% relative humidity and 25 ℃. Three measurements were taken, and the average result was noted.

2 Results and Discussion

2.1 Effect of dissolution conditions

The effect of dissolution temperature and dissolution time on the properties of ACCs were investigated.

2.1.1 Effect of dissolution temperature

Figure 2(a) shows the FTIR spectra of ACCs prepared at different dissolution temperatures. The ACCs prepared at dissolution temperatures of 25, 0 and −18 ℃ are denoted as ACC-25, ACC-0 and ACC-N18, respectively. The composites are mainly comparable to the untreated ACC, suggesting that the basic structure has been retained. The stretching vibration of O—H, and the characteristic cellulose peaks in a range of 2 990–3 660 cm^{-1} are present in the original cellulose. The O—H stretching vibration (3 335 cm^{-1}) shifts to a higher wavenumber (3 383 – 3 391 cm^{-1}) in the FTIR spectrum of ACCs. The decrease in the overall strength of hydrogen bonds between hydroxyl groups is the cause of this shift. In ACCs prepared at different dissolution temperatures, the absorption band at 1 430 cm^{-1}, associated with the —CH_2 shear motion, is weakened and moves to a lower wavenumber (1 423 – 1 427 cm^{-1}), indicating the change from cellulose Ⅰ to cellulose Ⅱ[18-20]. Additionally, the disappearance of the band at 1 105 cm^{-1} also indicates that cellulose Ⅰ is converted into cellulose Ⅱ[21-22]. Generally, the dissolution process is non-derivative, and the chemical constitution of the dissolved cellulose remains unchanged. Therefore, the obtained composites are truly "all-cellulose", as confirmed by the absence of a phosphorous peak in the EDS plot shown in Fig. 2(b).

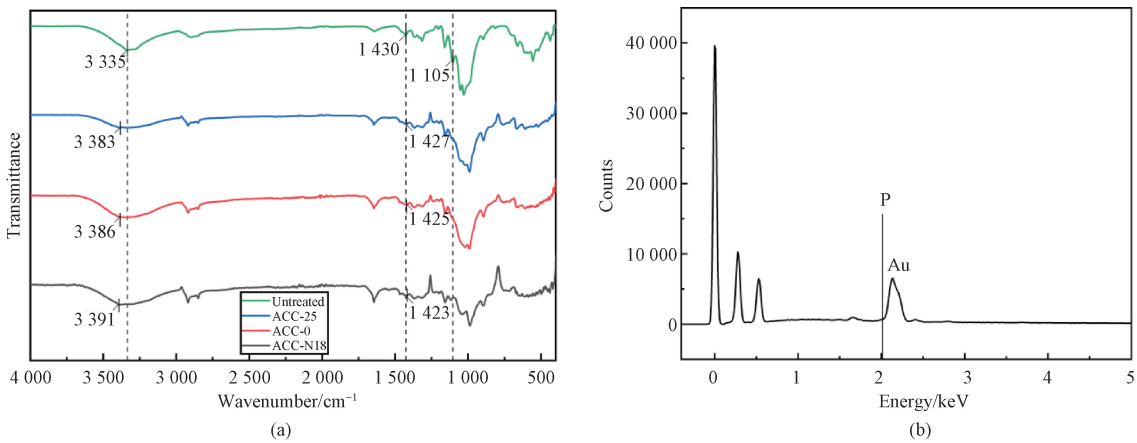

Fig. 2 Spectroscopic analysis of ACCs: (a) FTIR spectra of ACCs prepared at different dissolution temperatures; (b) EDS analysis of a representative ACC

Figure 3 (a) shows the XRD patterns of ACCs prepared at different dissolution temperatures. The dissolution time was 60 min. Non-crystalline scattering in ACCs increases with the decrease of dissolution temperature, suggesting wood pulp is being dissolved, forming more non-crystalline regions in the matrix phase. The crystalline structure of cellulose I is represented by peaks at 15.9° and 22.6°. However, large peaks at 2θ of 15.9° and 22.6° persist in all the XRD patterns of ACCs, indicating the presence of undissolved cellulose. As shown in Fig. 3, at a constant dissolution time of 60 min, the intensity of crystalline peaks decreases steadily with decreasing dissolution temperature. As the dissolution temperature is decreased from 25 to −18 ℃, the degree of crystallinity decreases from 76% to 72%, suggesting enhanced dissolution rates at lower temperatures. The crystallite size of ACCs is, in general, lower than that of the untreated ACC and also shows a positive correlation with dissolution temperature, where it is 2.5 nm for the ACC prepared at 25 ℃ and 2.2 nm for the ACC prepared at −18 ℃. Lower dissolution temperature results in more matrix phases in each composite layer and progressively decreases the undissolved fibers. Further studies were conducted at a dissolution temperature of −18 ℃, which was fast for cellulose dissolution and the formation of a sufficient matrix.

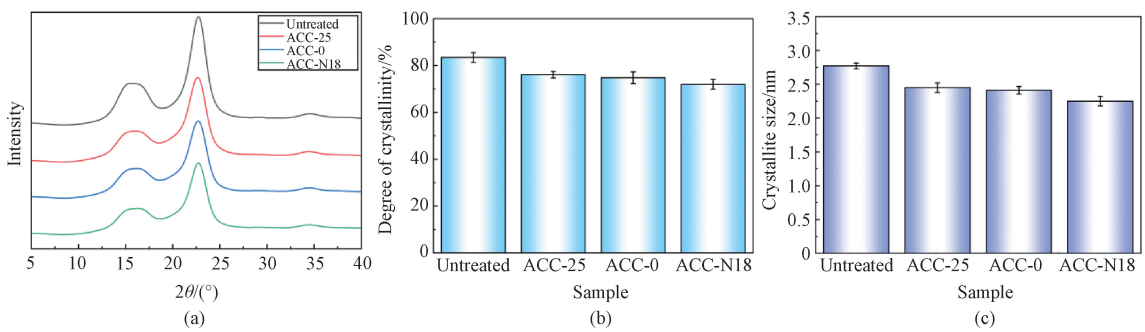

Fig. 3 Crystallinity analysis of ACCs prepared at different dissolution temperatures: (a) XRD patterns; (b) degrees of crystallinity; (c) crystallite sizes

2.1.2 Effect of dissolution time

Figure 4 shows the SEM images of ACCs at dissolution time between 0 and 60 min. The original sheet of wood pulp has a porous and open structure. For the untreated wood pulp, the fibers are pulled out. Since the matrix is insufficient to bind all nearby fibers, some pulled-out fiber layers can also be seen from ACCs prepared at a dissolution time of 15 min. Some voids between the fibers are still visible. After a dissolution time of 15 min, the matrix is formed from the outer sections of the fibers, binding neighbouring fibers together. After dissolution for 30 min, the failure mode shifts from fiber layer pullout to fiber breakage, demonstrating improved mechanical properties due to the fibers' improved interaction with the cellulose matrix[23]. When the dissolution time is extended to 45 min, the matrix volume increases as the amount of voids and undissolved fibers in the composites is notably reduced, indicating enhanced interaction of the two phases in ACCs. As a result, beyond 45 min of dissolution time, the fibrous structure transforms into a denser and more tightly bound structure. When the dissolution time is extended to 60 min, the fiber size is reduced, and

thicker matrix layers between the undissolved fiber cores are created[24]. Cellulose fibers in dense cellulose mats with a low porosity and a high interfiber contact exhibit visible breaking[25-26].

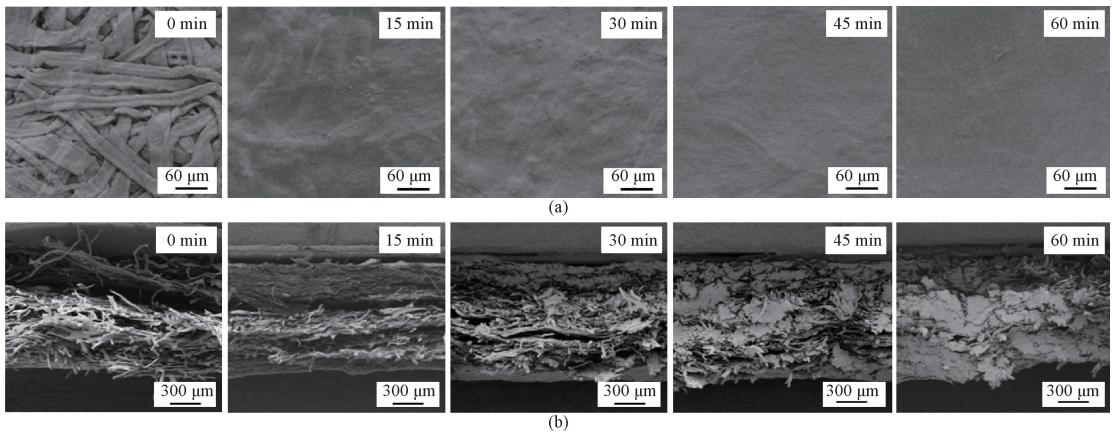

Fig. 4 Micromorphological analysis of ACCs prepared at −18 ℃ and different dissolution time: (a) SEM images of surface; (b) SEM images of cross section

Figure 5(a) displays the XRD patterns of ACCs prepared at different dissolution time. The cellulose fibers undergo a progressive rise in dissolution as the dissolution time increases, resulting in the transformation of the fibers into non-crystalline regions in the composite. The degrees of crystallinity and crystallite sizes of ACCs prepared at different dissolution time of 15, 30, 45 and 60 min are shown in Figs. 5(b) and 5(c). The intensity of the crystalline peaks in ACCs reduces as the dissolution time increases. After dissolution for 15 min, the ACC exhibits a lower degree of crystallinity of 79%, in comparison to the original wood pulp, which has a degree of crystallinity of 83%. The degree of crystallinity of the ACC is reduced to 77% after dissolution for 30 min. The degrees of crystallinity are 75% and 72% after dissolution for 45 and 60 min, respectively. The crystallite size of the original wood pulp is 2.8 nm, and after dissolution for 15 min, the crystallite size of the ACC is 2.7 nm. After dissolution for 15 and 30 min, the crystallite sizes decrease to 2.5 and 2.4 nm, respectively. After dissolution for 60 min, a minimum of 2.2 nm is observed. As suggested by the SEM images in Fig. 4, the reduction in the degree of crystallinity is accompanied by a decrease in fiber diameter and growth of the matrix phase[19].

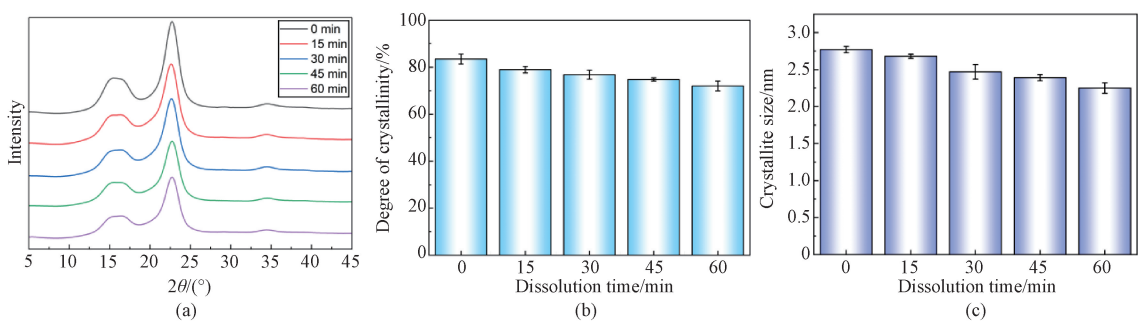

Fig. 5 Crystallinity analysis of ACCs prepared at −18 ℃ and different dissolution time: (a) XRD patterns; (b) degrees of crystallinity; (c) crystallite sizes

The degree of crystallinity decreases with the dissolution time for ACCs. The cellulose fibers experience a disruption of their intermolecular bonds, which are responsible for maintaining the crystalline structure. As the dissolution time increases, this disruption becomes more pronounced, leading to a progressive dissolution of crystalline regions into amorphous or non-crystalline regions. The cellulose molecules are reorganized in a less ordered manner without forming new derivatives, which reduces the degree of crystallinity[11, 24, 27]. Partially dissolved cellulose contains both cellulose Ⅰ and cellulose Ⅱ crystalline structures[19, 28-29]. XRD analysis further supports this transformation by showing a decrease in the peak intensity, which is one of the key indicators of the cellulose Ⅰ to cellulose Ⅱ transformation[30-32]. While the peak positions typical of cellulose I remain largely unchanged, the reduced intensity points to a transformation process where the cellulose structure is becoming more disordered, involving a coexistence of cellulose Ⅰ and cellulose Ⅱ phases[33].

Figure 6 shows the impact of the dissolution time on the mechanical properties of ACCs. The wood pulp has an elastic modulus of 0.7 GPa and a tensile strength of 16.0 MPa. The findings demonstrate that as the dissolution time reaches 15 min, the tensile strength of ACCs increases from 16.0 to 21.4 MPa. After dissolution for 15 min, the elongation at break and elastic modulus are 10.1% and 0.9 GPa, respectively. As the dissolution time increases to 45 min, the tensile strength and elastic modulus increase to 32.3 MPa and 1.3 GPa, respectively. The mechanical properties of ACCs exhibit a progressive increase with dissolution time of less than 45 min compared to the wood pulp. This implies that the treatment successfully enhances ACCs' mechanical properties. Beyond 45 min, despite a continual increase in the elongation at break, the tensile strength and elastic modulus fall back to 25.7 MPa and 1.1 GPa, respectively. The initial enhancement in mechanical properties of ACCs with dissolution time could be attributed to the ACCs' improved reinforcement-matrix bonding and the cellulose matrix's adequate capacity to fill the spaces between the fibers[20]. With prolonged dissolution time to 60 min, over-dissolution of the cellulose leads to a severe reduction of the reinforcement phase[8], leading to inferior tensile properties. The reinforcement phase of the cellulose fibers maintains a degree of structural integrity within the composite, allowing for effective stress transfer from the matrix to the fibers. Therefore, 45 min is the optimal dissolution time that gives the high mechanical properties due to sufficient matrix formation that allows enough stress transfer.

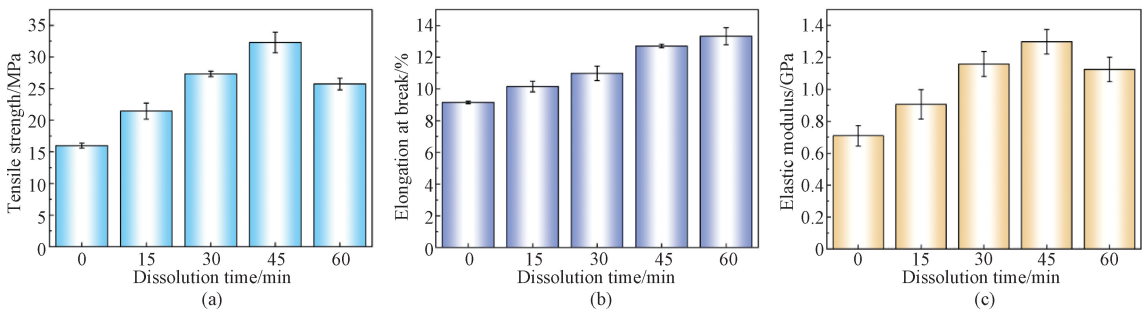

Fig. 6 Effect of dissolution time on mechanical properties of ACCs: (a) tensile strength; (b) elongation at break; (c) elastic modulus

The SEM study confirms the mechanical results, indicating that the tensile strength is higher when the dissolution time is 45 min. However, when the dissolution time is increased to 60 min, the tensile strength and the elastic modulus decrease. This is caused by the ineffective transmission of stress from the matrix to the reinforcement, resulting from the excessive quantity of matrix material formed. It is important to note that in these composites, the process of stress transfer from the matrix to the reinforcement is crucial, and the main mechanism controlling the mechanical properties of the cellulose mats is the binding between fibers[34-35].

2.2 Effect of coagulation bath

Figure 7(a) shows the O—H stretching vibration of ACCs prepared at −18 ℃ and a dissolution time of 45 min in aqueous H_3PO_4 and coagulated with three different coagulation baths (aqueous EtOH solutions with EtOH mass fractions of 0, 50% and 100%, denoted as ACC-E0, ACC-E50 and ACC-E100, respectively) followed by hot pressing at a load of 3000 kg. A clear change in the FTIR spectra of ACCs is the shift of the O—H stretching vibration caused by an increase in the total number of hydrogen bonds between hydroxyl groups. The —OH stretching vibration peak of the 50% EtOH solution exhibits the highest shift to the lower wavenumber of 3368 cm^{-1}. This suggests that the 50% EtOH solution generates the strongest hydrogen bonding interactions between cellulose chains, leading to the most ordered composite. Furthermore, it supports the optimal mass ratio of EtOH to water is 50∶50. In contrast, the ACC prepared by using a 100% EtOH coagulation bath shows a smaller shift to a lower wavenumber of 3387 cm^{-1}. This higher wavenumber compared to the 50% EtOH solution indicates reduced hydrogen bonding interactions and a less ordered structure in a pure ethanol coagulation bath.

Figures 7(b) – 7(d) show the effect of the coagulation bath on the mechanical properties of ACCs. The result of evaluating the mechanical properties of ACCs aligns with the findings of the FTIR spectra. The maximum tensile strength of 49.3 MPa is achieved when the mass fraction of EtOH is 50%. As the mass fraction of EtOH is further increased to 100 %, the tensile strength decreases significantly. The situation is the same for elongation at break and elastic modulus. Therefore, a mass fraction of 50% EtOH coagulation bath is chosen. The tensile strength of fully dissolved cellulose film is 40.4 MPa, which is lower than that of the ACC made from a 50% EtOH coagulation bath.

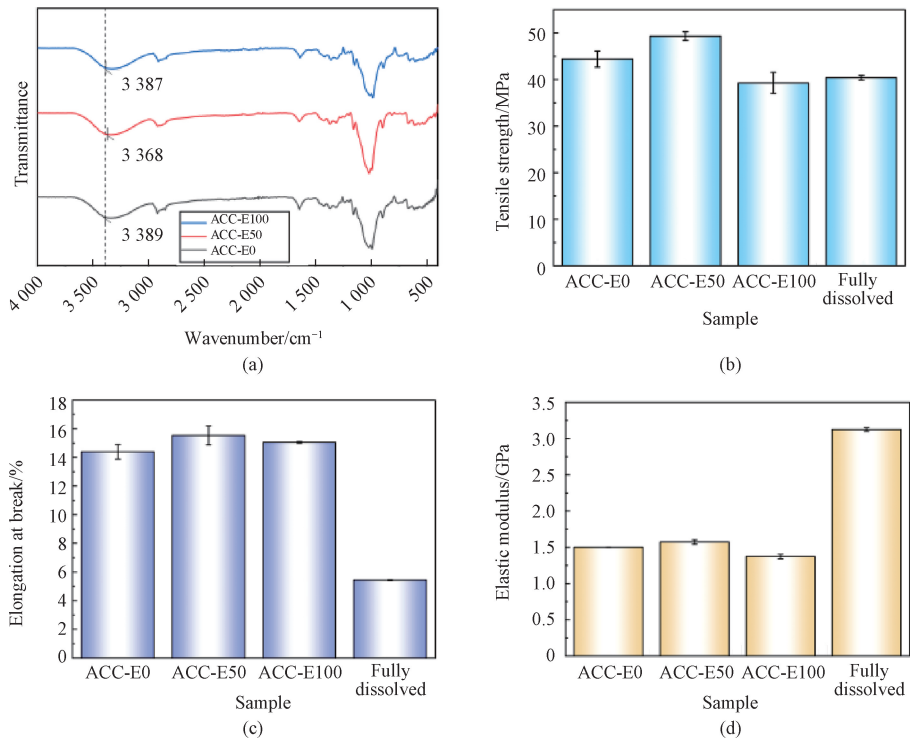

Fig. 7 Effect of coagulation bath on ACCs: (a) FTIR spectra; (b) tensile strength; (c) elongation at break; (d) elastic modulus

2.3 Effect of post-coagulating pressing

2.3.1 Effect on thermal properties

Figure 8(a) shows the thermal behavior of ACCs prepared at −18 ℃ and a dissolution time of 45 min in aqueous H_3PO_4 and hot-pressed at different pressing loads. The degradation process can be observed in three distinct stages. Both untreated wood pulp and ACCs have the first mass loss at about 100 ℃ due to the release of absorbed water[36]. The second stage, which takes place at temperatures ranging from 275 to 385 ℃, is responsible for the degradation process of the composites. Strong interfacial bonding can improve heat transfer and thermal stability[19, 37]. As pressing loads increase, the thermal stability of ACCs increases because higher loads can lead to a more compact and denser microstructure. This densification can enhance thermal stability as the material can withstand higher temperatures before decomposing. The third stage is characterized by the formation of charred residues, which takes place in a temperature range of 385 to 800 ℃. The DTG analysis (Fig. 8(b)) shows that all ACCs decompose at a slightly lower temperature compared with the untreated wood pulp, while increased pressing load leads to a notable increase in the decomposition temperature, likely due to densification and enhanced interfacial binding at higher pressing loads.

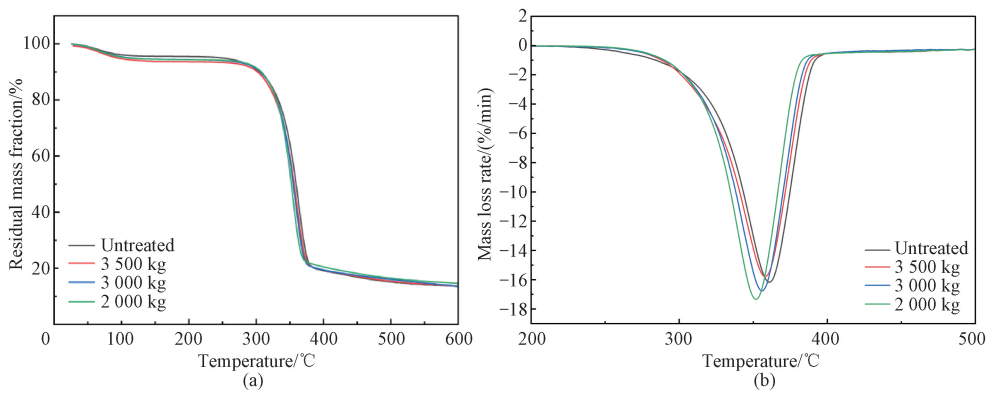

Fig. 8 Effect of pressing load on thermal properties of ACCs: (a) TG analysis curves; (b) DTG analysis curves

2.3.2 Effect on mechanical properties

Figure 9 shows the impact of post-coagulating pressing on the mechanical properties of ACCs prepared at −18 ℃ and a dissolution time of 45 min in

aqueous H_3PO_4 and hot pressed at different pressing loads. Higher loads can lead to a more compact and dense microstructure. With increasing pressing load, the mechanical properties of ACCs improved, indicating good interfacial adhesion and a decrease in stress concentrations and gaps that can lead to crack formation. The ACC prepared at a pressing load of 3 000 kg has a tensile strength and an elongation at break of 44.4 MPa and 14.4%, respectively. At a pressing load of 3 500 kg, the tensile strength and elongation at break drop significantly to 31.4 MPa and 11.8%, respectively, while elastic modulus remains mostly unchanged. Higher pressing loads generally enhance the densification of ACCs. When the pressing load increases beyond an optimal point, the cellulose fibers become overly compacted. This excessive load leads to a detrimental effect, causing excessive compaction that disrupts the interfacial bonding within the composite, reduces the effective stress transfer, and ultimately leads to low tensile strength. Therefore, 3 000 kg is the optimal hot pressing load with high mechanical properties.

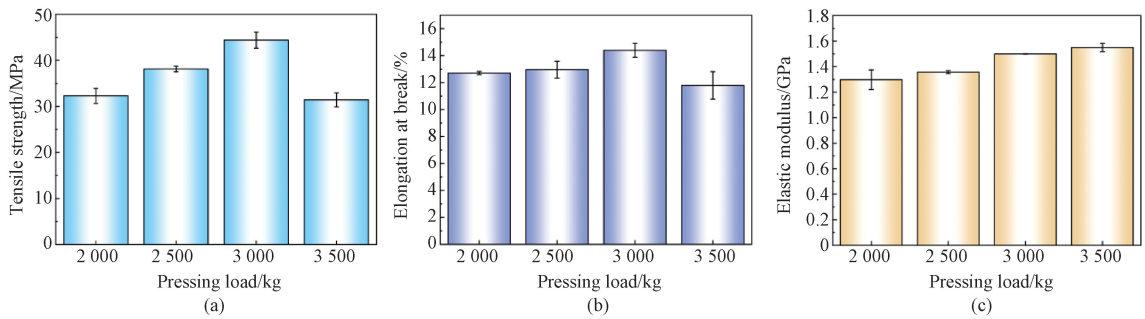

Fig. 9 Effect of pressing load on mechanical properties of ACCs: (a) tensile strength; (b) elongation at break; (c) elastic modulus

The mechanical properties of ACCs prepared by using the optimized conditions are compared with those previously reported in the literature in Table 1. The results show that ACCs prepared utilizing H_3PO_4 compared favorably with those prepared by other methods in terms of the tensile strength and elongation at break.

Table 1 Mechanical properties of ACCs previously reported and prepared in this work

Solvent	Type of cellulose	Tensile strength/MPa	Elastic modulus/GPa	Elongation at break/%	Dissolution method	Ref.
NaOH/urea	Bleached pine pulp	39.4	3.8	4.0	PD	[23]
LiCl/DMAc	Pineapple leaf microfiber	42.8	1.2	27	PD	[19]
$ZnCl_2$	Bleached pine pulp	53.9	4.7	3.6	PD	[38]
NaOH/urea	Softwood wood pulp	52.4	5.8	1.8	PD	[39]
LiCl/DMAc	Oil palm empty fruit bunches pulp	35.78	2.63	19.22	PD	[20]
NaOH/urea/H_2O	Bleached kraft bagasse pulp	10	0.5	6	PD	[30]
$BzMe_3NOH$	Bleached softwood pulp	38	6.3	6.4×10^{-3}	PD	[40]
H_3PO_4	Wood pulp	40.4	3.1	5.4	Full dissolution	This work
H_3PO_4	Wood pulp	49.3	1.6	15.5	PD	This work

2.4 Application properties of ACCs toward packaging material

Figure 10 (a) shows how the resistance to air permeation is improved in ACCs prepared at −18 ℃ and a dissolution time of 45 min in aqueous H_3PO_4 and hot pressed at different pressing loads. The untreated wood pulp (pressing load of 0) has the highest air permeability value of 5.6 mm/s, and it is reduced to 1.1 mm/s at the maximum pressing load of 3 500 kg. The reduction in macro pores resulting from the formation of a continuous cellulose Ⅱ matrix phase is responsible for the observed decrease in air permeability. Generally, a higher pressing load is favourable to the formation of densely packed composites that are good at retarding the air permeability.

As shown in Fig. 10(b), the surface of ACCs becomes less hydrophilic as the pressing load increases. Initially, the untreated wood pulp shows a low WCA of 56.7° due to its loose structure and the intrinsic hydrophilicity of cellulose[27], while the WCAs for all ACCs tested are above 80.0° and show an increasing trend with the pressing load. The observed trend can be understood similarly to the air barrier property, which improves due to the formation of a compact and dense matrix-fiber complex. The maximum WCA of 110.3° is achieved by using a high pressing load of 3 500 kg, which is notably higher than the values of ACC films previously reported by Pang et al. (54°)[41] and Han et al. (55°)[42], showing good potential to be used in packaging.

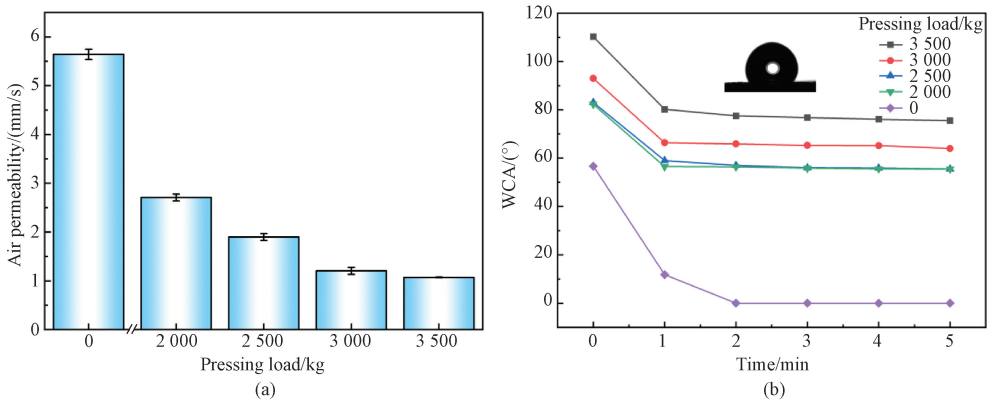

Fig. 10 Effect of pressing load on packaging related performance of ACCs: (a) air permeability; (b) surface hydrophobicity

3 Conclusions

This study explored the preparation and characterization of ACCs by utilizing cryogenic aqueous H_3PO_4 as a solvent. Fast and controllable dissolution of cellulose in aqueous H_3PO_4 at lower temperatures was achieved without chemical modification of the cellulose structure. Morphological analysis showed the significant impact of different dissolution time on the formation of the cellulose matrix and fiber interaction, and a dissolution time of 45 min was shown to yield the best matrix-to-filler ratio. The ACC prepared at a pressing load of 3 000 kg and coagulated with 50% EtOH solution showed the highest tensile strength of 49.3 MPa and elastic modulus of 1.6 GPa. As pressing loads increased, the thermal stability of ACCs increased because higher pressing loads could lead to a more compact and dense microstructure. The ACC obtained at a pressing load of 3 500 kg demonstrated the lowest air permeability of 1.1 mm/s and the highest WCA of 110.3°, showing great potential to be used as packaging materials. The study underlines the influence of the dissolution temperature, dissolution time, pressing load and EtOH mass fraction on the properties of ACCs, contributing to the advancement of cellulose-based materials for packaging applications.

References

[1] GHOLAMPOUR A, OZBAKKALOGLU T. A review of natural fiber composites: properties, modification and processing techniques, characterization, applications [J]. *Journal of Materials Science*, 2020, 55(3): 829-892.

[2] MALMSTRÖM E, CARLMARK A. Controlled grafting of cellulose fibres: an outlook beyond paper and cardboard [J]. *Polymer Chemistry*, 2012, 3(7): 1702-1713.

[3] ABDUL KHALIL H P S, BHAT A H, IREANA YUSRA A F. Green composites from sustainable cellulose nanofibrils: a review[J]. *Carbohydrate Polymers*, 2012, 87(2): 963-979.

[4] KALIA S, DUFRESNE A, CHERIAN B M, et al. Cellulose-based bio-and nanocomposites: a review [J]. *International Journal of Polymer Science*, 2011, 2011(1): 837875.

[5] TANPICHAI S, BOONMAHITTHISUD A, SOYKEABKAEW N, et al. Review of the recent developments in all-cellulose nanocomposites: properties and applications [J]. *Carbohydrate Polymers*, 2022, 286: 119192.

[6] GEORGOPOULOS S T, TARANTILI P A, AVGERINOS E, et al. Thermoplastic polymers reinforced with fibrous agricultural residues[J]. *Polymer Degradation and Stability*, 2005, 90(2): 303-312.

[7] NISHINO T, MATSUDA I, HIRAO K. All-cellulose composite[J]. *Macromolecules*, 2004, 37(20): 7683-7687.

[8] LI J Y, NAWAZ H, WU J, et al. All-cellulose composites based on the self-reinforced effect [J]. *Composites Communications*, 2018, 9: 42-53.

[9] BAGHAEI B, SKRIFVARS M. All-cellulose composites: a review of recent studies on structure, properties and applications [J]. *Molecules*, 2020, 25(12): 2836.

[10] HUBER T, BICKERTON S, MÜSSIG J, et al. Solvent infusion processing of all-cellulose composite materials[J]. *Carbohydrate Polymers*, 2012, 90(1): 730-733.

[11] DUCHEMIN B J C, NEWMAN R H, STAIGER M P. Structure-property relationship of all-cellulose composites[J]. *Composites Science and Technology*, 2009, 69(7/8): 1225-1230.

[12] SU H, WANG B J, SUN Z Q, et al. High-tensile regenerated cellulose films enabled by unexpected enhancement of cellulose dissolution in cryogenic aqueous phosphoric acid [J]. *Carbohydrate Polymers*, 2022, 277: 118878.

[13] ZAVREL M, BROSS D, FUNKE M, et al.

High-throughput screening for ionic liquids dissolving (ligno-) cellulose [J]. *Bioresource Technology*, 2009, 100(9): 2580-2587.
[14] ZHU S D, WU Y X, CHEN Q M, et al. Dissolution of cellulose with ionic liquids and its application: a mini-review [J]. *Green Chemistry*, 2006, 8(4): 325-327.
[15] SEYMOUR R B, STAHL G A. Macromolecular solutions: solvent-property relationships in polymers [M]. New York: Elsevier, 2013.
[16] LI J H, HAO Z Z, WANG B J, et al. High-tensile chitin films regenerated from cryogenic aqueous phosphoric acid [J]. *Carbohydrate Polymers*, 2023, 312: 120826.
[17] QIAO T, YANG C L, ZHAO L Y, et al. High tensile regenerated cellulose fibers via cyclic freeze-thawing enabled dissolution in phosphoric acid for textile-to-textile recycling of waste cotton fabrics[J]. *International Journal of Biological Macromolecules*, 2024, 277: 133911.
[18] OOSTHUIZEN H, DU TOIT E L, LOOTS M T, et al. A novel cost-effective choline chloride/ionic liquid solvent for all-cellulose composite production[J]. *Cellulose*, 2023, 30(1): 127-140.
[19] TANPICHAI S, WITAYAKRAN S. All-cellulose composites from pineapple leaf microfibers: structural, thermal, and mechanical properties[J]. *Polymer Composites*, 2018, 39(3): 895-903.
[20] JAAFAR M Z, RIDZUAN F F M, KASSIM M H M, et al. The role of dissolution time on the properties of all-cellulose composites obtained from oil palm empty fruit bunch[J]. *Polymers*, 2013, 15(3): 691.
[21] REDDY K O, MAHESWARI C U, DHLAMINI M S, et al. Preparation and characterization of regenerated cellulose films using *Borassus* fruit fibers and an ionic liquid [J]. *Carbohydrate Polymers*, 2017, 160: 203-211.
[22] LIU Z H, SUN X F, HAO M Y, et al. Preparation and characterization of regenerated cellulose from ionic liquid using different methods [J]. *Carbohydrate Polymers*, 2015, 117: 99-105.
[23] HILDEBRANDT N C, PILTONEN P, VALKAMA J P, et al. Self-reinforcing composites from commercial chemical pulps via partial dissolution with NaOH/urea[J]. *Industrial Crops and Products*, 2017, 109: 79-84.
[24] SOYKEABKAEW N, ARIMOTO N, NISHINO T, et al. All-cellulose composites by surface selective dissolution of aligned ligno-cellulosic fibres[J]. *Composites Science and Technology*, 2008, 68(10/11): 2201-2207.
[25] SOYKEABKAEW N, SIAN C, GEA S, et al. All-cellulose nanocomposites by surface selective dissolution of bacterial cellulose[J]. *Cellulose*, 2009, 16(3): 435-444.
[26] PLACKETT D, ANTURI H, HEDENQVIST M, et al. Physical properties and morphology of films prepared from microfibrillated cellulose and microfibrillated cellulose in combination with amylopectin [J]. *Journal of Applied Polymer Science*, 2010, 117(6): 3601-3609.
[27] ADAK B, MUKHOPADHYAY S. All-cellulose composite laminates with low moisture and water sensitivity[J]. *Polymer*, 2018, 141: 79-85.
[28] SIRVIÖ J A, VISANKO M, HILDEBRANDT N C. Rapid preparation of all-cellulose composites by solvent welding based on the use of aqueous solvent[J]. *European Polymer Journal*, 2017, 97: 292-298.
[29] LENNHOLM H, IVERSEN T. Estimation of cellulose Ⅰ and Ⅱ in cellulosic samples by principal component analysis of ^{13}C-CP/MAS-NMR-spectra[J]. *hfsg*, 1995, 49(2): 119-126.
[30] ABOU-YOUSEF H, KAMEL S. Physico-mechanical properties of all-cellulose composites prepared by different approaches from micro-fibrillated bagasse pulp fibers [J]. *Materials Today Communications*, 2023, 35: 105672.
[31] BARANOV A, SOMMERHOFF F, DUCHEMIN B, et al. Toward a facile fabrication route for all-cellulose composite laminates via partial dissolution in aqueous tetrabutylphosphonium hydroxide solution [J]. *Composites Part A: Applied Science and Manufacturing*, 2021, 140: 106148.
[32] WEI Q Y, LIN H, YANG B, et al. Structure and properties of all-cellulose composites prepared by controlling the dissolution temperature of a NaOH/urea solvent[J]. *Industrial & Engineering Chemistry Research*, 2020, 59(22): 10428-10435.
[33] DUCHEMIN B J C, MATHEW A P, OKSMAN K. All-cellulose composites by partial dissolution in the ionic liquid 1-butyl-3-methylimidazolium chloride[J]. *Composites Part A: Applied Science and Manufacturing*, 2009, 40(12): 2031-2037.
[34] TANPICHAI S, SAMPSON W W, EICHHORN S J. Stress-transfer in microfibrillated cellulose reinforced poly (lactic acid) composites using Raman spectroscopy [J]. *Composites Part A: Applied Science and Manufacturing*, 2012, 43(7): 1145-1152.
[35] ALMGREN K M, GAMSTEDT E K, NYGÅRD P, et al. Role of fibre-fibre and fibre-matrix adhesion in stress transfer in composites made from resin-impregnated paper sheets [J]. *International Journal of Adhesion and Adhesives*, 2009, 29(5): 551-557.
[36] YOUSEFI H, MASHKOUR M, YOUSEFI R. Direct solvent nanowelding of cellulose fibers to make all-cellulose nanocomposite[J]. *Cellulose*,

2015, 22: 1189-1200.
[37] ARÉVALO R, PICOT O T, WILSON R M, et al. All-cellulose composites by partial dissolution of cotton fibres [J]. *Journal of Biobased Materials and Bioenergy*, 2010, 4(2): 129-138.
[38] TERVAHARTIALA T, HILDEBRANDT N C, PILTONEN P, et al. Potential of all-cellulose composites in corrugated board applications: comparison of chemical pulp raw materials [J]. *Packaging Technology and Science*, 2018, 31(4): 173-183.
[39] PILTONEN P, HILDEBRANDT N C, WESTERLIND B, et al. Green and efficient method for preparing all-cellulose composites with NaOH/urea solvent [J]. *Composites Science and Technology*, 2016, 135: 153-158.
[40] HU Y C, HU F Q, GAN M X, et al. A rapid, green method for the preparation of cellulosic self-reinforcing composites from wood and bamboo pulp [J]. *Industrial Crops and Products*, 2021, 169: 113658.
[41] PANG J H, LIU X, WU M, et al. Fabrication and characterization of regenerated cellulose films using different ionic liquids [J]. *Journal of Spectroscopy*, 2014, 2014(1): 214057.
[42] HAN D L, YAN L F. Preparation of all-cellulose composite by selective dissolving of cellulose surface in PEG/NaOH aqueous solution [J]. *Carbohydrate Polymers*, 2010, 79(3): 614-619.

低温磷酸水溶液部分溶解木浆制备全纤维素复合材料

METASEBIA Gizaw[1], 王碧佳[1,2*], 冯雪凌[1,2], 荣立夺[1,2]

1. 东华大学 化学与化工学院, 上海 201620
2. 东华大学 国家染整工程技术研究中心, 上海 201620

摘　要: 全纤维素复合材料（all-cellulose composite, ACC）是利用未衍生纤维素同时作为基质和增强相的复合材料。ACC 完全由纤维素构成，由于增强相和基质具有完全相同的化学性质，从而使它们能解决生物复合材料中纤维−基质黏附性差的问题。该研究利用低温磷酸水溶液部分溶解木浆制备 ACC，探究了溶解温度、溶解时间和压力负荷对 ACC 性能的影响。结果表明，溶解时间为 45 min 能获得最优的增强相−基质比例。使用乙醇质量分数为 50%的乙醇水溶液作为凝固浴，并在干燥过程中施加 3 000 kg 压力负荷，能获得力学性能好的 ACC，拉伸强力和弹性模量分别达到 49.3 MPa（比木浆板提高约 210%）和 1.6 GPa（比木浆板提高约 122%）。复合材料的致密性影响 ACC 的力学性能。透气性分析表明，ACC 的阻隔性能也显著优于木浆板，采用 3 500 kg 的压力负荷，能使表面水接触角升高至 110.3°（比木浆板提高约 94%），透气性显著降低至 1.1 mm/s，显示了其在绿色包装材料领域良好的应用前景。

关键词: 纤维素；全纤维素复合材料；低温磷酸；部分溶解；可持续材料